VSV-EBOV Induces Temporal and Dose-Dependent Transcriptional Responses in Non-human Primates

Amanda N. Pinski[1], Kevin J. Maroney[1], Andrea Marzi[2] and Ilhem Messaoudi[1,3,4]*

[1] Department of Molecular Biology and Biochemistry, University of California, Irvine, Irvine, CA, United States, [2] Laboratory of Virology, Division of Intramural Research, National Institute of Allergy and Infectious Diseases, National Institutes of Health, Rocky Mountain Laboratories, Hamilton, MT, United States, [3] Center for Virus Research, University of California, Irvine, Irvine, CA, United States, [4] Institute for Immunology, University of California, Irvine, Irvine, CA, United States

Zaire Ebola virus (EBOV), the causative agent of Ebola virus disease (EVD), is a member of the *Filoviridae* family. EVD is characterized by innate and adaptive immune dysregulation that leads to excessive inflammation, coagulopathy, lymphopenia, and multi-organ failure. Recurrent outbreaks of EBOV emphasize the critical need for effective and deployable anti-EBOV vaccines. The FDA-approved VSV-EBOV vaccine protects non-human primates (NHPs) and humans from EBOV when given at a 10–20 million PFU dose. We recently demonstrated that a dose as small as 10 PFU protected NHPs from lethal EBOV infection. Furthermore, 1 PFU of VSV-EBOV protected 75% of vaccinated NHPs. In this study, we performed a comparative transcriptional analysis of the whole blood transcriptome in NHPs vaccinated with doses of VSV-EBOV associated with complete protection (10M PFU), protection with mild EVD (10 PFU), and break-through protection (1 PFU) before and after challenge with a lethal dose of EBOV Makona. Transcriptional findings demonstrated that, regardless of dose, vaccination significantly attenuated the upregulation of genes associated with fatal EVD. Genes involved in T- and B-cell activation were more highly expressed in groups receiving 10 or 10M PFU than in 1 PFU–vaccinated animals. Furthermore, the singular vaccinated (1 PFU) non-survivor exhibited a transcriptional signature distinct from both surviving vaccinated animals and controls that received an irrelevant vaccine. These findings provide additional insight into mechanisms of vaccine-mediated protection and informing public policy on vaccine distribution during outbreaks.

Keywords: EBOV, transcriptomics, non-human primate, vaccine, ervebo protection, VSV-EBOV

INTRODUCTION

Zaire Ebola virus (EBOV), a member of the *Filoviridae* family, causes Ebola virus disease (EVD) (1, 2). EVD is characterized by excessive inflammation, aberrant coagulation, and severe lymphopenia due to dysregulated activation of innate and adaptive immunity, culminating in multi-organ failure and death (2, 3). Non-survivors exhibit cellular and transcriptional signatures of exaggerated apoptosis, a cytokine storm, and rampant myeloid cell activation (4–11). Depending on the strain of EBOV, case fatality rates range from 40 to 90% (12, 13). Few successful antivirals, therapeutics, and vaccines preventing or treating EVD have been approved for human use (14, 15).

The 2013–2016 West Africa EBOV Makona epidemic and the recent EBOV outbreaks in the Democratic Republic of the Congo (DRC) and Guinea highlight the urgent need to understand mechanisms of anti-EBOV immunity and vaccine-mediated protection (13, 16, 17).

VSV-EBOV (also known as rVSV-EBOV-GP, Ervebo by Merck) is the only FDA-approved EBOV vaccine to date (12, 18). Composed of a replication-competent vesicular stomatitis virus (VSV) pseudotyped with the EBOV glycoprotein (GP), this vaccine shows high efficacy in both non-human primate (NHP) models and humans (19–24). NHPs are considered the gold standard model for EBOV disease given their accurate recapitulation of human pathobiology (24–26). A single dose [10 million (10M) PFU] of VSV-EBOV administered to NHPs 28 days before lethal challenge with the EBOV Makona or Kikwit strains completely protects animals from disease (21, 23, 27, 28). These animals develop robust humoral responses targeting the EBOV GP, which is believed to be a correlate of protection (12, 28). VSV-EBOV also acts therapeutically, partially protecting NHPs when vaccinated 3 days (67% survival) before or several hours (33–67% survival) after EBOV exposure (27, 29–31). In humans, phase I and II clinical studies demonstrated robust safety of this vaccine in children, adolescents, adults, pregnant women, and immunocompromised individuals at doses ranging from 3×10^5 PFU to 20M PFU (32–36). VSV-EBOV received FDA approval in 2019 after two phase III ring-vaccination trials conducted during the West Africa epidemic showed nearly 100% efficacy with a single dose of 20M PFU (37–44).

The dual function of VSV-EBOV as a prophylactic and rapid-acting, therapeutic vaccine represents a critical public health strategy for outbreak control. Administering lower, yet equally effective, doses of VSV-EBOV can facilitate vaccine distribution during outbreaks and evade adverse side effects associated with high doses (33, 43, 45, 46). We recently showed that NHPs vaccinated with as little as dose as 10^4 PFU were completely protected from EVD (19). Furthermore, animals receiving a dose as small as 10 PFU— ∼1 millionth the FDA-approved dose—experienced mild EVD but were completely protected from fatal disease. Moreover, 75% of NHPs vaccinated with 1 PFU succumbed to infection. The molecular mechanisms surrounding this dose-dependent efficacy remain unknown, but critical for understanding VSV-EBOV-mediated protection and anti-EBOV immunity.

In this study, we performed a transcriptional analysis of historical whole blood samples collected from NHPs vaccinated with either the fully protective 10M PFU dose of VSV-EBOV or doses associated with full protection against fatal disease (10 PFU), or break-through protection (1 PFU) (19). Expression of genes associated with EVD (e.g., inflammation, apoptosis, myeloid cell mobilization) were downregulated in vaccinated NHPs in a dose-dependent manner. Canonical genes involved in B- and T-cell activation were most highly expressed in animals receiving 10 or 10M PFU of VSV-EBOV. The animal vaccinated with 1 PFU and succumbing to challenge exhibited transcriptional signatures intermediate of vaccinated counterpart and controls. Collectively, these findings suggest a critical role for dosage in VSV-EBOV-mediated immunity and protection during EBOV infection.

MATERIALS AND METHODS

Study Design

Whole blood–derived RNA samples were leveraged from a previous study (19). All infectious work with EBOV was performed in the maximum containment laboratory at the Rocky Mountain Laboratories (RML), Division of Intramural Research, National Institute of Allergy and Infectious Diseases, National Institutes of Health. RML is an AAALAC-accredited institution. All procedures followed standard operating procedures approved by the Institutional Biosafety Committee. Animal work was performed in strict accordance with the recommendations described in the Guide for the Care and Use of Laboratory Animals of the National Institute of Health, the Office of Animal Welfare and the Animal Welfare Act, United States Department of Agriculture. The study was approved by the Institutional Animal Care and Use Committee (IACUC). Procedures were conducted in animals anesthetized by trained personnel under the supervision of veterinary staff. The humane endpoint criteria for euthanasia were specified and approved by the IACUC. All efforts were made to ameliorate animal welfare and minimize animal suffering in accordance with the Weather all report on the use of non-human primates in research (https://royalsociety.org/policy/publications/2006/weatherall-report/).

In brief, RNA was extracted from whole blood of animals vaccinated with either VSV-EBOV (1 PFU, 10 PFU, or 10M PFU) or VSV-MARV (10M PFU) before vaccination (d28), following vaccination (d14) and following challenge (d6, d28, d42) as previously described. Animals were challenged with a lethal dose (1,000 PFU) of EBOV-Makona in the caudal thighs. Animals were monitored daily for signs of disease and behavioral changes.

cDNA Library Construction

Quality and quantity of RNA were determined using an Agilent 2100 Bioanalyzer. cDNA libraries were constructed using the NEB Next Ultra II Direction RNA Library Prep Kit (Thermo Fisher). RNA was treated with RNase H and DNase I following depletion of ribosomal RNA (rRNA). Adapters were ligated to cDNA products and the subsequent ∼300–400 base pair (bp) amplicons were PCR amplified and selected by size exclusion. All cDNA libraries were assessed for quality and quantity prior to 100 bp single-end sequencing using the Illumina NovaSeq platform.

Bioinformatics Analysis

Preliminary data analysis was performed with RNA-Seq workflow module of systemPipeR, developed by Backman and Girke (47). RNA-Seq reads were demultiplexed, quality-filtered, and trimmed using Trim Galore (average Phred score cut-off of 30, minimum length of 50 bp). FastQC was used to generate quality reports. Alignment was performed with hisat2 using reference genome *Macaca*

fascicularis (Macaca_fascicularis.Macaca_fascicularis_5.0.dna.-toplevel.fa) and annotation file Macaca_fascicularis.Macaca_fascicularis_5.0.94.gtf for annotation. Raw expression values (gene-level read counts) were generated using the summarizeOverlaps function and normalized (read per kilobase of transcript per million mapped reads, rpkm) using the edgeR package. Statistical analysis with edgeR was used to determine differentially expressed genes (DEGs) meeting the following criteria: genes with average rpkm of ≥ 1, an FDR corrected $p \leq 0.05$, and a $|\log_2 \text{fold change}| \geq 1$ compared with either untreated animals (d28) or control-vaccinated animals at 6 days post-challenge. Two-way forward regression analysis was performed with MaSigPro (48). DESeq2 analysis without biological replicates was used to compare the dose 1 non-survivor ($n = 1$) with the control animals ($n = 2$) at d6. The fold change (dose 1 non-survivor relative to average of controls) was calculated using the exactTest function. A $|\log_2 \text{fold change}| \geq 3$ cut-off was used to identify significant protein-coding genes (SGs) with notably higher or lower expression in the dose 1 non-survivor. Genes exhibiting dose-dependent regulation were determined using Short Time-Series Expression Miner (STEM) (49).

Functional enrichment of DEGs was performed using Metascape to identify relevant gene ontology (GO) biological process terms and immunological signatures (50). Heatmaps, bubbleplots, Venn diagrams, and beanplots were generated using R packages ggplot2 and VennDiagrams. GO network plots were generated in Cytoscape (version 3.5.1). Bar graphs and statistics were generated using GraphPad Prism software (version 8).

Digital cell quantification was performed using ImmQuant with the IRIS database, which includes transcriptional profiles from 22 immune cell types in normal human blood (51). This algorithm predicts changes in immune cell frequencies within heterogeneous populations, including whole blood and lymphoid tissue, using bulk transcriptional data. Human references were used given the close genetic homology between NHPs and humans as well the fact that NHP recapitulate clinical hallmarks of Ebola virus disease (52, 53).

Statistical Analysis

Differences in predicted changes in immune cell frequencies was determined using one-way ANOVA. $^*p \leq 0.05$, $^{**}p \leq 0.01$, $^{***}p \leq 0.001$, and $^{****}p \leq 0.0001$.

RESULTS

Overview of Study Cohort

To elucidate mechanisms of protection regulating dose-dependent protection mediated by VSV-EBOV, we leveraged historical RNA samples from our previous study (19). In brief, 12 macaques were randomly divided among three groups receiving one of three different doses of VSV-EBOV at baseline (d28): 10M PFU ($n = 4$), 10 PFU ($n = 4$), and 1 PFU ($n = 4$). NHPs were challenged 28 days after vaccination with a lethal dose (1,000 PFU) of EBOV Makona, Guinea C07 strain (EBOV-Makona). Nearly all NHPs receiving 1 PFU (100%) or 10 PFU (75%) developed viremia. One 1 PFU-vaccinated NHP succumbed to infection. In addition, two macaques were vaccinated with the
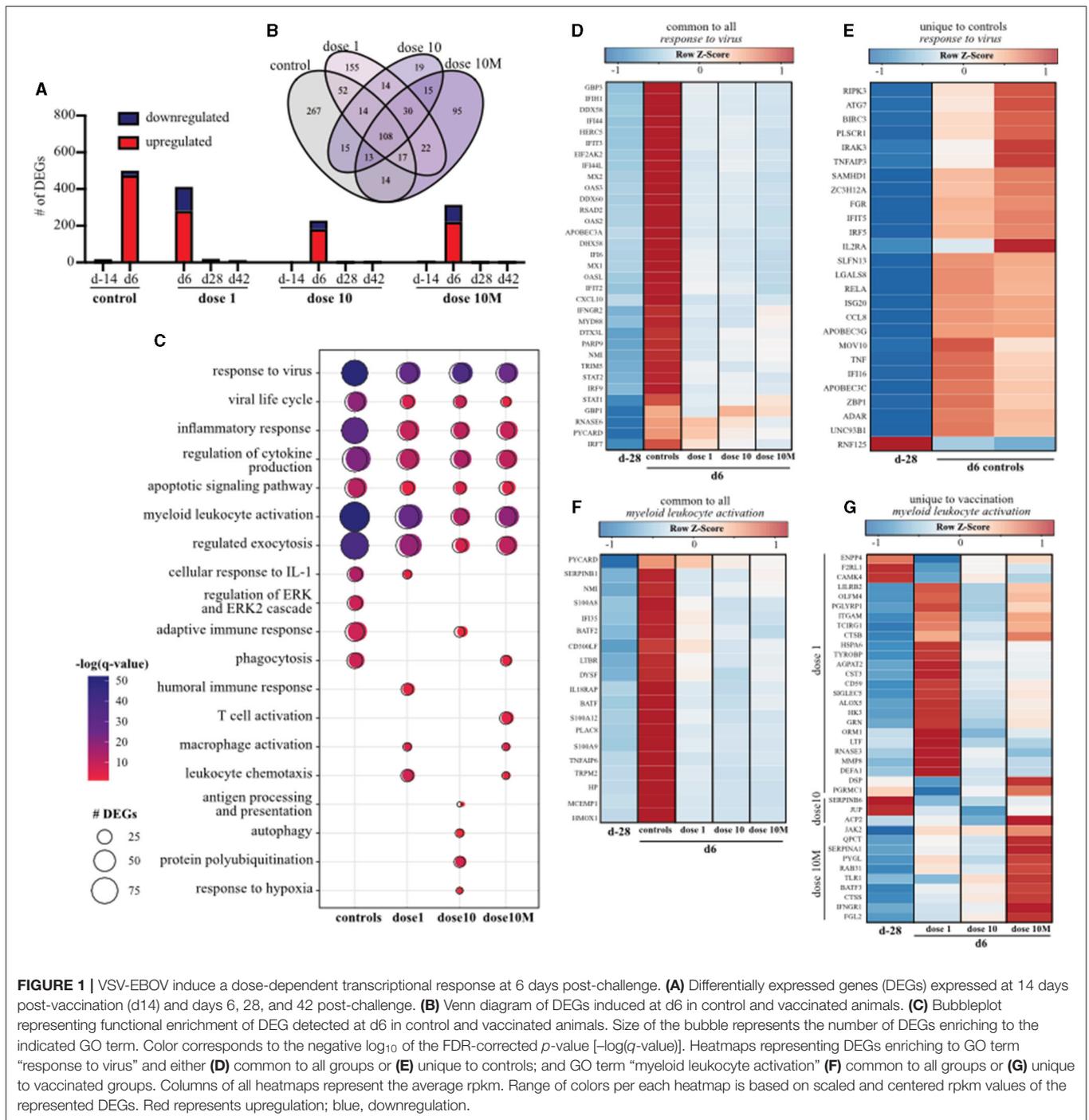
Marburg GP-vectored rVSV vaccine (VSV-MARV), which does not protect animals from EBOV (23, 27, 28). These animals were euthanized at d6 and d7 post-challenge when clinical scores reached humane euthanasia levels. RNA was extracted from whole blood collected before vaccination (d28), 2 weeks after vaccination (d14; dose 10, dose 10M, control), and d6, d28, and d42 post-challenge (all doses). We performed RNA sequencing on all these samples to determine global changes in gene expression.

Transcriptional Responses to EBOV Makona Challenge Are Overlapping Among VSV-EBOV–Vaccinated Animals

We compared samples taken post-vaccination (d14) and post-challenge (d6, d28, d42) to baseline samples collected at d28 to quantify DEGs (**Figure 1**). The non-survivor was excluded from this analysis. Principal component analysis (PCA) demonstrated a clear separation between d6 and remaining samples (**Supplementary Figure 1A**). Consistent with previous studies and PCA, we detected very few DEGs (e.g., control, $n = 18$) to no DEGs (e.g., dose 10, dose 10M) 2 weeks after vaccination and 4–6 weeks after lethal EBOV challenge for all groups (**Figure 1A**). The greatest induction of DEGs occurred at d6, with the controls exhibiting the largest number of DEGs ($n = 500$) (**Figure 1B**). Most DEGs were upregulated. A core of 108 DEGs was shared by all groups at d6 (**Figure 1B**). These genes enriched to immunological pathways such as "naïve B cell vs. plasmablast up" (e.g., *LGALS3BP*), "TREG vs FOXP3 KO TREG precursor DN" (*SOCS3*), and "IFN-alpha vs. IFN-gamma stim macrophage up" (*STAT1*) (**Supplementary Figure 1B**).

To understand the biological relevance of DEGs, we performed functional enrichment of DEGs induced at d6 in each group (**Supplementary Figure 1C**, **Figure 1C**). DEGs detected d6 enriched to GO terms reflecting hallmarks of EVD: antiviral defense (e.g., "response to virus"), inflammation (e.g., "inflammatory response"), cell death (e.g., "apoptotic signaling pathway"), and innate immunity (e.g., "myeloid leukocyte activation") (**Figure 1C**). The number of DEGs and the significance of the enrichment were significantly larger in the control group compared with the vaccinated groups (**Figure 1C**). Gene expression changes associated with inflammation, like "cellular response to IL-1" and "regulation of ERK/2 cascade" GO terms, were only observed in controls and dose 1. GO terms associated with antigen presentation (e.g., "autophagy," "antigen processing and presentation;" *MR1*, *PSMB8*, *TAP1*) were unique to dose 10. DEGs enriching to GO terms associated with T-cell activation were only seen in the dose 10M group (**Figure 1C**).

We next examined the magnitude of expression for DEGs enriching to GO terms illustrating EVD (**Figures 1D–G**). DEGs enriching to GO term "response to virus" and shared by all groups included canonical components of type I/II interferon (IFN) signaling (e.g., *IFNGR2*, *STAT1*, *STAT2*), nucleic acid sensors (e.g., *DDX58*, *DHX58*), and interferon stimulated genes (ISGs) (e.g., *EIF2AK2*, *RNASE6*) (**Figure 1D**). These DEGs were significantly more highly upregulated in controls compared with vaccinated animals. Additional DEGs detected only in controls

FIGURE 1 | VSV-EBOV induce a dose-dependent transcriptional response at 6 days post-challenge. **(A)** Differentially expressed genes (DEGs) expressed at 14 days post-vaccination (d14) and days 6, 28, and 42 post-challenge. **(B)** Venn diagram of DEGs induced at d6 in control and vaccinated animals. **(C)** Bubbleplot representing functional enrichment of DEG detected at d6 in control and vaccinated animals. Size of the bubble represents the number of DEGs enriching to the indicated GO term. Color corresponds to the negative $\log_{10}$ of the FDR-corrected p-value [$-\log(q$-value)]. Heatmaps representing DEGs enriching to GO term "response to virus" and either **(D)** common to all groups or **(E)** unique to controls; and GO term "myeloid leukocyte activation" **(F)** common to all groups or **(G)** unique to vaccinated groups. Columns of all heatmaps represent the average rpkm. Range of colors per each heatmap is based on scaled and centered rpkm values of the represented DEGs. Red represents upregulation; blue, downregulation.

that enriched to "response to virus" included genes that play roles in viral RNA editing (e.g., *ADAR*, *APOBEC3G*) and inflammation (e.g., *FGR*, *RIPK2*) (**Figure 1E**). Similarly, DEGs that mapped to "myeloid leukocyte activation" GO term and detected in all groups were also more highly upregulated in the controls. Notable genes within this set included *IL18RAP*, *S100A8*, and *S100A12*, which are important for neutrophil activation and inflammation (**Figure 1F**). Some DEGs enriching to "myeloid

cell activation" were only detected in VSV-EBOV–vaccinated animals (**Figure 1G**). These included *CD59* and *MMP8* that play a role in complement-mediated immunity (dose 1), *SERPINB6* important for (dose 10), and BATF3 and *JAK2* important for myeloid cell differentiation (dose 10M) (**Figure 1G**). The 20 upregulated DEGs detected in dose 10M and enriching to "T cell activation" primarily regulated T-cell activity (e.g., *ARG2*, *IDO1*, *CD274*, *TNFAIP8L2*).

Transcriptional Indicators Reflecting Hallmarks of EVD Are Attenuated in Protected Animals

To better understand how VSV-EBOV dose modulates responses to EBOV, we directly compared VSV-EBOV–vaccinated NHPs with control-vaccinated NHPs at peak infection (d6) (**Figure 2A**). We detected similar numbers of DEGs for dose 1 ($n = 629$) and dose 10 ($n = 699$) while a smaller number of DEGs ($n = 499$) were detected in dose 10M (**Figure 2A**). The majority of DEGs were downregulated and shared among all VSV-EBOV-vaccinated groups, indicating that these genes were upregulated in fatal disease (**Figure 2B**). DEGs from each group enriched to similar GO terms notably "myeloid leukocyte activation," "neutrophil degranulation," "response to virus," and "leukocyte migration" (**Figure 2C**). DEGs detected only in the dose 1 group additionally mapped to cell death pathways ("necrotic cell death") and oxidative stress (e.g., "reactive oxygen

species metabolic process") (**Figure 2C**). DEGs detected only in higher vaccine doses groups (10 and 10M PFU) enriched to "response to IFN-γ".

DEGs enriching to "response to virus" included ISGs (e.g., *IFI27*, *ISG20*), NFKB signaling pathway members (e.g., *IKBKB/E*, *RELA*), and genes regulating mature virion production (e.g., *BST2*, *EIF2AK2*, *OAS2*) (**Supplementary Figure 1C**). The majority of DEGs enriching to "myeloid leukocyte activation" played a role in monocyte activation (e.g., *CD14*, *CD68*), coagulation (e.g., *PLAU*, *PLAUR*), and inflammation (e.g., *CCL3*, *CLEC4D/5A*, *S100A8*) (**Supplementary Figure 1D**). Important differences between controls and dose 10–vaccinated animals include increased expression of several MHC class II molecules (e.g., *HLA-DMB*, *HLA-DRB5*) and other genes critical for T-cell activation and differentiation (e.g., *CD3E/G*, *LY9*, *THEMIS*, *TRACT*, *TRAT1*, *ZAP70*) (**Supplementary Figure 1E**). Lastly, the DEGs belonging to GO terms unique to dose 1 animals
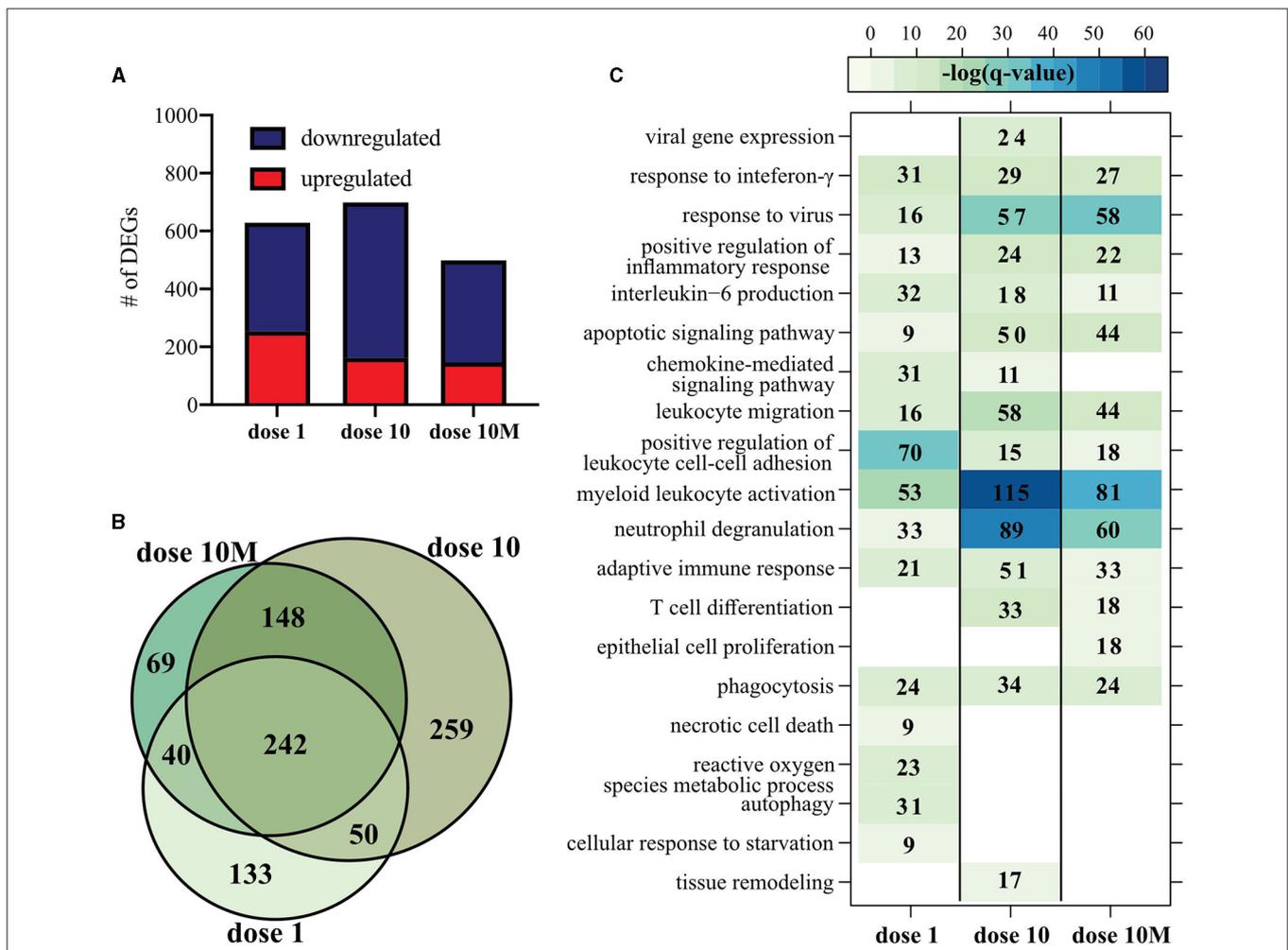

FIGURE 2 | Comparison of vaccinated animals to controls at peak infection illustrates attenuated disease. **(A)** DEGs detected at 6 days post-challenge in vaccinated animals relative to controls. **(B)** Venn diagram of DEGs in **(A)**. **(C)** Functional enrichment of DEGs in **(A)**. Color intensity represents statistical significance as the negative log of the FDR-adjusted *p*-value [–log(*q*-value)], with range of colors based on the GO terms with the lowest and highest statistical value for all GO terms present. Blank boxes indicate lack of statistical significance. Numbers of DEGs enriching to each GO term are noted in each box.

were mainly downregulated factors modulating oxidative stress (e.g., *NFE2L2*, *RIPK2*, *VMP1*) (**Supplementary Figure 1F**). Upregulated DEGs encoded hemoglobin subunits (e.g., *HBA1/2*, *HBM*, *HBQ1*) (**Supplementary Figure 1F**).

Since whole blood samples were not available for flow cytometry, we used our transcriptomic data to perform digital cell quantification with the IRIS database to predict changes in immune cell frequencies (**Supplementary Figure 1G**) (51, 54). B- and T-cell lymphopenia was predicted for all groups at d6, including vaccinated animals. Reduced frequencies of memory B cells were more significant in the dose 1 group vaccinated non-survivor, and less pronounced in the dose 10 and 10M vaccine groups. While activated monocyte populations (monocyte d1/7) were more significantly increased in the control at d6, less dramatic increases were predicted for dose 10 and dose 10M. Dendritic cell and neutrophil populations were also predicted to increase at d6, but not significantly for neutrophils. Cell frequencies were predicted to return to baseline at d28 for all surviving animals.

Genes Involved in B- and T-cell Activation Are Upregulated in Dose-Dependent Manner in Vaccinated Animals at Peak Infection

We next identified clusters of genes that exhibited dose-dependent regulation among vaccinated groups at d6 using STEM with dose as a variable instead of time (**Figure 3**) (49). We determined three clusters of genes (**Figure 3A**). Expression of the genes in clusters 1 and 2 increased in a dose-dependent manner. In contrast, genes in cluster 3 were most highly expressed in dose 1–vaccinated animals. Genes in cluster 1 enriched to GO terms associated with adaptive immunity (e.g., "lymphocyte activation," "T cell differentiation") (**Figure 3B**). Genes in cluster 1 included canonical genes involved in T-cell activation (e.g., *CD2*, *CD28*, *CD3D*, *CD8A*, *ICOS*, *IL7R*) and B-cell-mediated immunity (e.g., *LCK*, *IGHG2*, *SLAMF7*), as well as indicators of cellular cytotoxicity (e.g., *KLRD1*, *KLRK1*) (**Figure 3C**). Genes playing roles in cellular cytotoxicity such as *PRF1* and *CD69*, and inflammation mediated by monocytes/macrophages like *CCR5* and *CD36*, were part of cluster 2 (**Figure 3D**). In contrast, genes in cluster 3 enriched to GO terms associated with innate immunity and inflammation (e.g., "myeloid leukocyte activation," "coagulation") (**Figure 3B**). Components of the complement pathway (e.g., *C1QB*), neutrophil-mediated immunity (e.g., *CD99*, *S100A8*), and acute inflammatory response (e.g., *CD163*, *IL18R1*, *IL1R2*) belonged to cluster 3 (**Figure 3E**).

Dose 1 PFU VSV-EBOV-Vaccinated Non-survivor Exhibits a Distinct Transcriptional Signature From Survivors and Negative Controls

In the dose 1 group, one animal succumbed to infection while three survived. Therefore, we performed a two-way forward regression analysis to identify clusters of genes that were similarly and differently regulated following EBOV challenge between the non-survivors and survivors (**Figures 4A–D**). We identified two gene clusters (**Figure 4A**). Genes in cluster 1 were highly upregulated in the non-survivor at d6 compared with survivors. Functional enrichment of cluster 1 genes mapped to GO terms associated with antiviral defense, cellular stress, leukocyte activation, and intracellular vesicle mobilization (**Figure 4B**). Of the genes enriching to "response to virus" and "regulation of defense response," many were ISGs and viral restriction factors such as *HERC5*, *MX1*, and *SAMHD1* (**Figures 4B,C**). Genes that enriched to GO term "myeloid leukocyte activation" played a role in neutrophil-mediated immunity such as activation marker *CD177* and NETosis factor *S100A12*. This term also encompassed mediators of the complement pathway (e.g., *CD59* and *CD93*) and cell adhesion (e.g., *CAPZA1*, *OLFM4*) (**Figures 4B,C**). The 16 genes in cluster 2 were downregulated by the non-survivor but upregulated in the survivors from d6 to d28 (**Figures 4A,C**). These few genes included *CDC34* and *PSMD9* involved in protein degradation, *HYAL3* in maintenance of epithelial integrity, and *ICAM4* in cell migration (**Figures 4A,C**).

We next compared transcriptional profiles from the dose 1 non-survivor with control animals at d6 to elucidate molecular mechanisms differentiating fatal infections with and without VSV-EBOV vaccination (**Figure 4E**). Analysis with DESeq2 was performed given only that there was only one non-survivor and two control animals. We identified 163 significant genes (SGs) [$\log_2$(fold-change) cut-off of 3 in either direction] between the two groups. Most SGs (n=144) were downregulated in non-survivor compared with controls. Functional enrichment showed that these SGs belong to immune pathways regulating responses to vaccination (e.g., "day 3 vs. day 7 YF17D vaccine PBMC DN") and innate and adaptive immune cell responses to antigen (e.g., "untreated vs IFN-gamma stim macrophage UP") (**Figure 4E**). Several SGs belonging to these pathways are involved in leukocyte recruitment (e.g., *CCL3/4/7/8*, *CXCL10/11*), inflammatory innate immunity (e.g., *CD14*, *IFNB1*, *IL6*, *TNF*) and lymphocyte-mediated immunity (e.g., *IGKV-20*, *IL15RA*, *PRF1*, *SLAMF7*).

DISCUSSION

VSV-EBOV (rVSV-ZEBOV, Ervebo by Merck) is currently the only FDA-approved vaccine to protect against EVD. Human clinical trials initiated during the 2013–2016 West Africa epidemic and the 2018–2020 outbreak in the DRC demonstrated robust safety and efficacy, although vaccination was frequently associated with transient muscle pain, arthralgia, fever, and fatigue (43, 44). This is most likely due to high dose of the vaccine used in these vaccination campaigns. Recurrent EBOV outbreaks in endemic regions highlight the need to improve the availability of vaccines and resolve undesirable side effects in target populations without the loss of protective efficacy. Our previous study determined the dose-dependent efficacy of VSV-EBOV in cynomolgus macaques vaccinated 28 days before lethal EBOV challenge (19). We showed that complete protection is achieved with a dose of 10^6 PFU while doses ranging from 10
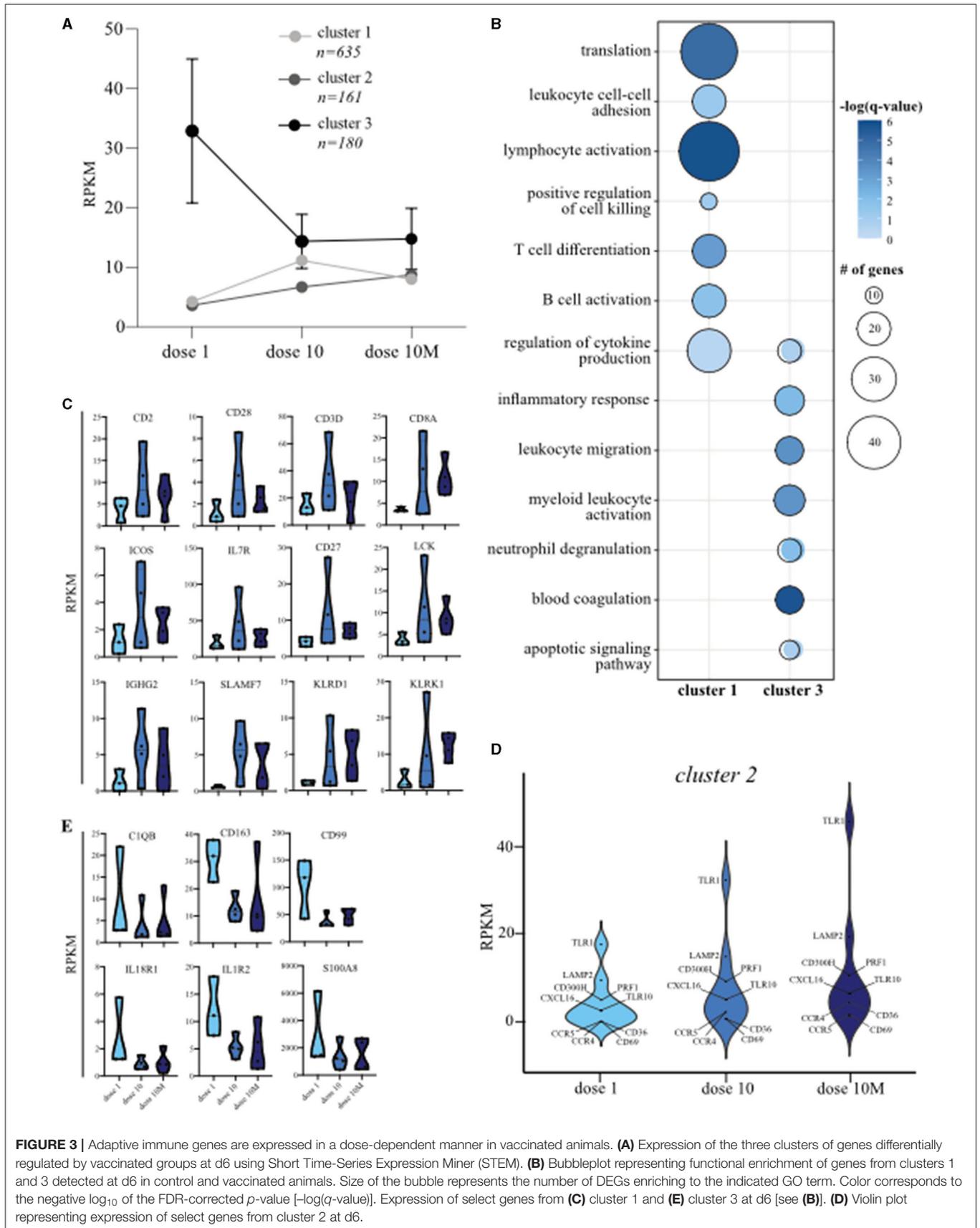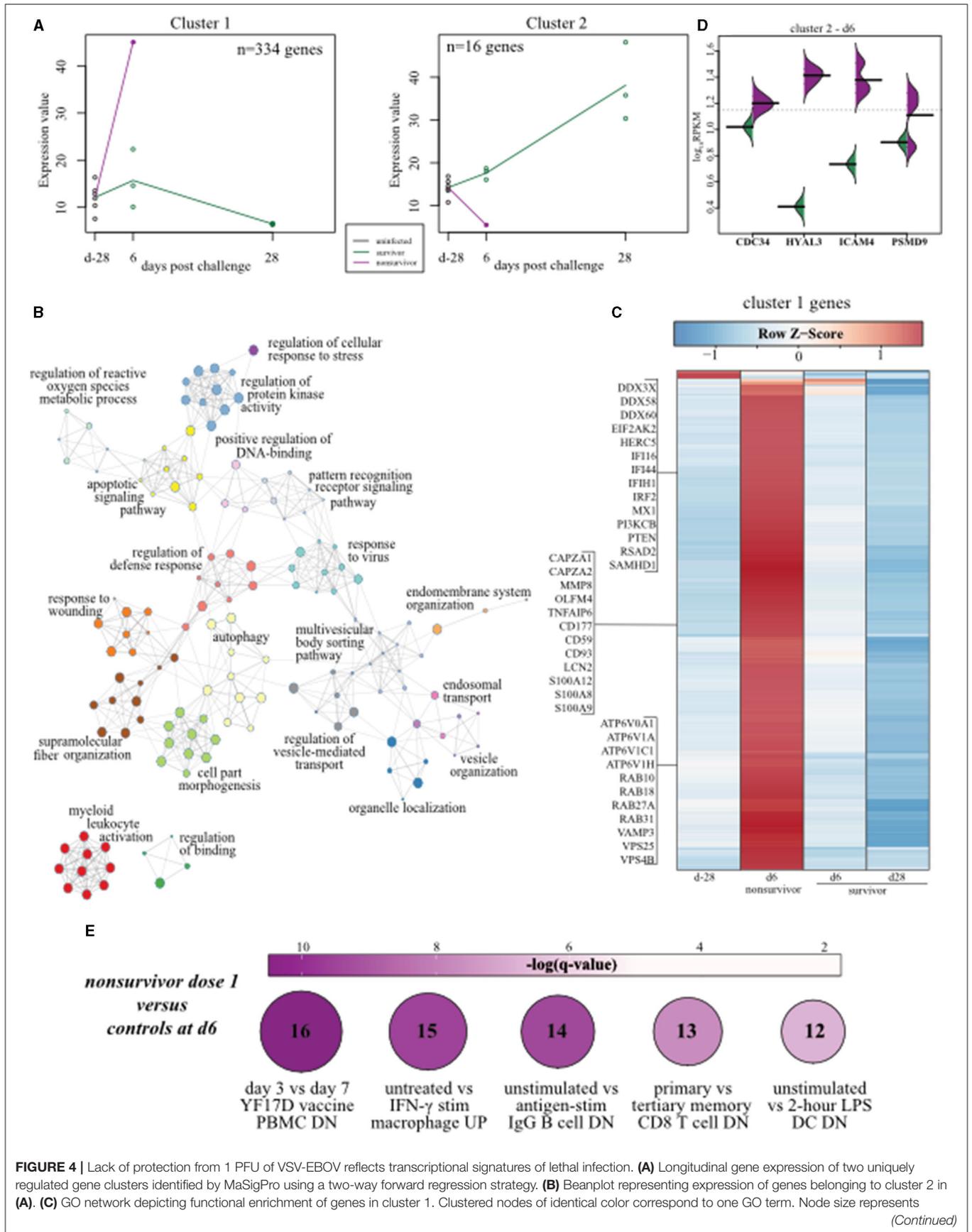
FIGURE 3 | Adaptive immune genes are expressed in a dose-dependent manner in vaccinated animals. **(A)** Expression of the three clusters of genes differentially regulated by vaccinated groups at d6 using Short Time-Series Expression Miner (STEM). **(B)** Bubbleplot representing functional enrichment of genes from clusters 1 and 3 detected at d6 in control and vaccinated animals. Size of the bubble represents the number of DEGs enriching to the indicated GO term. Color corresponds to the negative $\log_{10}$ of the FDR-corrected p-value [$-\log(q$-value)]. Expression of select genes from **(C)** cluster 1 and **(E)** cluster 3 at d6 [see **(B)**]. **(D)** Violin plot representing expression of select genes from cluster 2 at d6.

FIGURE 4 | Lack of protection from 1 PFU of VSV-EBOV reflects transcriptional signatures of lethal infection. **(A)** Longitudinal gene expression of two uniquely regulated gene clusters identified by MaSigPro using a two-way forward regression strategy. **(B)** Beanplot representing expression of genes belonging to cluster 2 in **(A)**. **(C)** GO network depicting functional enrichment of genes in cluster 1. Clustered nodes of identical color correspond to one GO term. Node size represents

(Continued)

FIGURE 4 | the number of DEGs associated with the GO term. Gray lines represent shared interaction between GO terms, with density and number indicating the strengths of connections between closely and distantly related GO terms. **(D)** Heatmap of DEGs belonging to cluster 1. Exemplar genes are highlighted. Columns of all heatmaps represent the average rpkm of survivors or untreated animals, and rpkm of the single non-survivor. Range of colors per each heatmap is based on scaled and centered rpkm values of the represented DEGs. Red represents upregulation; blue, downregulation. **(E)** Enrichment of the 163 significant genes [SGs, $|\log_2(\text{fold-change})| \geq 3$] regulated in the dose1 non-survivor relative to control animals at d6 as determined by DESeq2. Size of the bubble and written number indicates umber of enriching SGs. Color intensity represents statistical significance as the negative log of the FDR-adjusted p-value [$-\log(q$-value)], with range of colors based on the immunological signature terms with the lowest and highest statistical value for all immunological signatures present.

PFU to 10^4 PFU are sufficient to prevent severe EVD, but not viremia. On the other hand, 25% of animals receiving 1 PFU of VSV-EBOV succumbed to challenge and exhibited hallmarks of EVD. Here, we investigated the molecular mechanisms surrounding dose-dependent efficacy using transcriptomics with historical samples.

Interestingly, we observed functionally similar transcriptional response in vaccinated animals and control-vaccinated animals at d6. The transcriptional changes contained hallmarks of anti-viral responses including an induction of ISGs, myeloid cell activation factors, and apoptosis despite the absence of viremia in 10M PFU-vaccinated animals, suggesting that small amounts of antigen can trigger a robust response (4, 12, 55). However, the magnitude of induction was significantly higher in animals that succumbed to disease, as was previously reported for both NHP and humans, indicative of a dysregulated inflammatory response (4–6, 24, 56–60). Indeed, we previously reported lower plasma levels of IFNγ, IL-6, and TNFα, and stable levels of platelets and AST in vaccinated animals throughout challenge as compared with controls (19). Analysis of dose-dependent expression of genes also revealed a cluster of pro-inflammatory genes highly expressed in only dose 1–vaccinated animals.

We detected induction of genes involved in humoral immunity in dose 1–vaccinated animals during challenge, suggesting that infection may serve as an antigen "boost" since these animals initially presented with low antibodies. A similar transcriptional response including B-cell activation genes was previously seen in animals vaccinated with VSV-EBOV only 3 days before EBOV challenge (27, 61). The significant upregulation of genes important for regulatory T-cell function in dose 10M–vaccinated animals compared with controls suggests a controlled response to infection not seen in fatal NHP and human cases (46, 59, 62–64). Aberrant T-cell responses are associated with fatal EVD and immunological impairment during other viral diseases such as EBV reactivation in humans (59, 65, 66). Furthermore, we identified a cluster of genes that were significantly upregulated in dose 10– and 10M–vaccinated animals compared with dose 1 animals that included canonical members of T- and B-cell signaling pathways like *CD28* and *LCK*, as well as NK- and T-cell-mediated cytotoxicity. The role of humoral immunity is well-established for VSV-EBOV while the roles of NK- and T-cell-mediated immunity are less clear (12, 28, 67–69). Nonetheless, these findings indicate that VSV-EBOV dosage likely plays a key role in shaping nature and durability of long-term immunity, although future studies are needed to test this hypothesis.

Digital cell quantification demonstrated significant decreases in T- and B-cell subsets for all groups. This lymphopenia

could indicate two different processes in controls vs. vaccinated animals. Specifically, the reduced frequency of B and CD8 T cell could indicate (1) lymphocyte apoptosis in controls and (2) recruitment into tissues of vaccinated animals. This hypothesis is supported by the more significant upregulation of apoptotic genes in the control group. Monocytosis was predicted to be significant in the controls and animals that received lower vaccine doses. The downregulation of canonical neutrophil chemoattractant *CXCL8* in all vaccinated animals further suggests a lack of EVD-associated neutrophilia in these animals even though we did detect a greater expression of inflammatory and neutrophil-associated genes in dose 1, but not doses 10 and 10M, animals. Since lymphoid tissues serve as key sites of EBOV pathogenesis, future studies should address the impact of vaccine dose within these sites (1, 58).

Given that a single animal in the dose 1–vaccinated group succumbed to EBOV challenge, we had the opportunity to explore transcriptional signatures differentiating non-survivors from survivors within the same vaccine group as well as non-survivors from controls. Several hundred genes that play a critical role in inflammation and apoptosis were only upregulated by the non-survivor. These transcriptional changes may provide critical diagnostic markers. However, induction of canonical genes influencing myeloid and lymphocyte activation pathways/differentiation (e.g., *IFNB*) was less significant in the non-survivor compared with control-vaccinated animals. Therefore, vaccinated non-survivors are associated with intermediate transcriptional responses of protected NHPs and unvaccinated NHPs.

In summary, we determined a downregulation of EVD-related genes in vaccinated survivors and dose-related expression of key components of T- and B-cell-mediated immune responses. This supports the proposal for a reduction in vaccine dose to prevent adverse side effects and facilitate greater vaccine distribution in endemic regions, which represents a critical strategy for controlling ongoing outbreaks. However, there are several caveats to this study. First, the transcriptional findings reported here are restricted to whole blood and not cell specific. Second, we were unable to confirm the up- and downregulation of genes at the protein level, as well as changes in immune cell frequencies with flow cytometry. Third, the impact of dosage on durability of anti-EBOV immunity remains to be investigated. Future studies will focus on determining (1) the contributions of both innate and adaptive cells to dose-dependent immunity, (2) the durability of dose-dependent immunity, and (3) the therapeutic efficacy of lower doses of VSV-EBOV.

DATA AVAILABILITY STATEMENT

The datasets presented in this study can be found in online repositories. The names of the repository/repositories and accession number(s) can be found at: https://www.ncbi.nlm.nih.gov/, PRJNA747033.

ETHICS STATEMENT

The animal study was reviewed and approved by Rocky Mountain Laboratories (RML), Division of Intramural Research, National Institute of Allergy and Infectious Diseases, National Institutes of Health Institutional Animal Care and Use Committee.

AUTHOR CONTRIBUTIONS

AM and IM designed and conceived the study and wrote the article. AM, AP, and KM performed the experiments. AP, KM, and IM analyzed the data. All authors agreed to the final draft of the article.

FUNDING

ACKNOWLEDGMENTS

SUPPLEMENTARY MATERIAL

The Supplementary Material for this article can be found online at: https://www.frontiersin.org/articles/10.3389/fviro.2021.747198/full#supplementary-material

Supplementary Figure 1 | VSV-EBOV vaccination results in the downregulation of EVD-associated genes at peak disease. **(A)** Principal component analysis of control and vaccinated animals by day and treatment. **(B)** Functional enrichment of the 108 DEGs common to all vaccinated and control-vaccinated animals at 6 days post-challenge (DPC) in **Figure 1B** to immunological signatures. Color of bars represents the negative log of the FDR-adjusted p-value [–log(q-value)] while size correlates to number of DEGs enriching to the indicated signature. Heatmaps illustrating gene expression of DEGs from GO terms in **Figure 2C**: **(C)** "response to virus" and **(D)** "myeloid leukocyte activation." **(E)** Expression of T-cell-related DEGs using average RPKM. **(F)** Beanplots representing expression of DEGs from unique dose 1 GO terms in **Figure 2B**. **(G)** Predicted changes in immune cell frequencies at 6 and 28 DPC. Columns of all heatmaps represent the average rpkm or predicted cell frequency of the indicated group at 6 DPC. Range of colors for each heatmap is based on scaled and centered rpkm values of the represented DEGs. Red represents upregulation; blue, downregulation. One-way ANOVA conducted relative to untreated (d28) animals.

REFERENCES

1. Feldmann H, Geisbert TW. Ebola haemorrhagic fever. *Lancet.* (2011) 377:849–62. doi: 10.1016/S0140-6736(10)60667-8

2. Rivera A, Messaoudi I. Molecular mechanisms of ebola pathogenesis. *J Leukocyte Biol.* (2016) 100:889–904. doi: 10.1189/jlb.4RI0316-099RR

3. Jacob ST, Crozier I, Fischer WA, Hewlett A, Kraft CS, Vega, A, et al. Ebola virus disease. *Nat Rev Dis Primers.* (2020) 6:1–31. doi: 10.1038/s41572-020-0147-3

4. Liu X, Speranza E, Muñoz-Fontela C, Haldenby S, Rickett NY, Garcia-Dorival I, et al. Transcriptomic signatures differentiate survival from fatal outcomes in humans infected with Ebola virus. *Genome Biol.* (2017) 18:4. doi: 10.1186/s13059-016-1137-3

5. Eisfeld AJ, Halfmann PJ, Wendler JP, Kyle JE, Burnum-Johnson KE, Peralta Z, et al. Multi-platform 'omics analysis of human ebola virus disease pathogenesis. *Cell Host Microbe.* (2017) 22:817–29.e8. doi: 10.1016/j.chom.2017.10.011

6. Versteeg K, Menicucci AR, Woolsey C, Mire CE, Geisbert JB, Cross RW, et al. Infection with the makona variant results in a delayed and distinct host immune response compared to previous Ebola virus variants. *Sci Rep.* (2017) 7:9730. doi: 10.1038/s41598-017-09963-y

7. Wauquier N, Becquart P, Padilla C, Baize S, Leroy EM. Human fatal zaire ebola virus infection is associated with an aberrant innate immunity and with massive lymphocyte apoptosis. *PLoS Negl Trop Dis.* (2010) 4:e837. doi: 10.1371/journal.pntd.0000837

8. Baize S, Leroy EM, Georges AJ, Georges-Courbot MC, Capron M, Bedjabaga I, et al. Inflammatory responses in Ebola virus-infected patients. *Clin Exp Immunol.* (2002) 128:163–8. doi: 10.1046/j.1365-2249.2002.01800.x

9. Madelain V, Baize S, Jacquot F, Reynard S, Fizet A, Barron S, et al. Ebola viral dynamics in nonhuman primates provides insights into virus immuno-pathogenesis and antiviral strategies. *Nat Commun.* (2018) 9:4013. doi: 10.1038/s41467-018-06215-z

10. Cimini E, Viola D, Cabeza-Cabrerizo M, Romanelli A, Tumino N, Sacchi A, et al. Different features of Vδ2 T and NK cells in fatal and non-fatal human ebola infections. *PLOS Negl Trop Dis.* (2017) 11:e0005645. doi: 10.1371/journal.pntd.0005645

11. Bradfute SB, Swanson PE, Smith MA, Watanabe E, McDunn JE, Hotchkiss RS, et al. Mechanisms and consequences of ebolavirus-induced lymphocyte apoptosis. *J Immunol.* (2010) 184:327–35. doi: 10.4049/jimmunol.0901231

12. Pinski AN, Messaoudi I. To B or not to B: mechanisms of protection conferred by rVSV-EBOV-GP and the roles of innate and adaptive immunity. *Microorganisms.* (2020) 8:1473. doi: 10.3390/microorganisms8101473

13. CDC. *Outbreaks Ebola (Ebola Virus Disease).* CDC (2021). Available online at: https://www.cdc.gov/vhf/ebola/outbreaks/index-2018.html (accessed June 1, 2021).

14. Cross RW, Mire CE, Feldmann H, Geisbert TW. Post-exposure treatments for ebola and marburg virus infections. *Nat Rev Drug Discov.* (2018) 17:413–34. doi: 10.1038/nrd.2017.251

15. O'Donnell K, Marzi A. The ebola virus glycoprotein and its immune responses across multiple vaccine platforms. *Exp Rev Vaccines.* (2020) 19:267–77. doi: 10.1080/14760584.2020.1738225

16. CDC. *2014-2016 Ebola Outbreak in West Africa.* History Ebola (Ebola Virus Disease). CDC (2020). Available online at: https://www.cdc.gov/vhf/ebola/history/2014-2016-outbreak/index.html (accessed June 5, 2021).

17. NEJM. *After Ebola in West Africa—Unpredictable Risks, Preventable Epidemics.* NEJM (2020). Available online at: https://www.nejm.org/action/downloadFigures (accessed May 1, 2021).

18. Commissioner O. *First FDA-Approved Vaccine for the Prevention of Ebola Virus Disease, Marking a Critical Milestone in Public Health Preparedness and Response.* FDA. (2020). Available online at: https://www.fda.gov/news-events/

press-announcements/first-fda-approved-vaccine-prevention-ebola-virus-disease-marking-critical-milestone-public-health (accessed May 29, 2021).

19. Marzi A, Reynolds P, Mercado-Hernandez R, Callison J, Feldmann F, Rosenke R, et al. Single low-dose VSV-EBOV vaccination protects cynomolgus macaques from lethal ebola challenge. *EBioMedicine*. (2019) 49:223–31. doi: 10.1016/j.ebiom.2019.09.055

20. Qiu X, Fernando L, Alimonti JB, Melito PL, Feldmann F, Dick D, et al. Mucosal immunization of cynomolgus macaques with the VSVDeltaG/ZEBOVGP vaccine stimulates strong ebola GP-specific immune responses. *PLoS ONE*. (2009) 4:e5547. doi: 10.1371/journal.pone.0005547

21. Geisbert TW, Daddario-Dicaprio KM, Geisbert JB, Reed DS, Feldmann F, Grolla A, et al. Vesicular stomatitis virus-based vaccines protect nonhuman primates against aerosol challenge with ebola and marburg viruses. *Vaccine*. (2008) 26:6894–900. doi: 10.1016/j.vaccine.2008.09.082

22. Marzi A, Chadinah S, Haddock E, Feldmann F, Arndt N, Martellaro C, et al. Recently identified mutations in the ebola virus-makona genome do not alter pathogenicity in animal models. *Cell Rep*. (2018) 23:1806–16. doi: 10.1016/j.celrep.2018.04.027

23. Jones SM, Feldmann H, Ströher U, Geisbert JB, Fernando L, Grolla A, et al. Live attenuated recombinant vaccine protects nonhuman primates against ebola and marburg viruses. *Nat Med*. (2005) 11:786–90. doi: 10.1038/nm1258

24. Marzi A, Feldmann F, Hanley PW, Scott DP, Günther S, Feldmann H. Delayed disease progression in cynomolgus macaques infected with ebola virus makona strain. *Emerg Infect Dis*. (2015) 21:1777–83. doi: 10.3201/eid2110.150259

25. Baseler L, Chertow DS, Johnson KM, Feldmann H, Morens DM. The pathogenesis of ebola virus disease. *Ann Rev Pathol Mech Dis*. (2017) 12:387–418. doi: 10.1146/annurev-pathol-052016-100506

26. Geisbert TW, Hensley LE, Larsen T, Young HA, Reed DS, Geisbert JB, et al. Pathogenesis of ebola hemorrhagic fever in cynomolgus macaques: evidence that dendritic cells are early and sustained targets of infection. *Am J Pathol*. (2003) 163:2347–70. doi: 10.1016/S0002-9440(10)63591-2

27. Marzi A, Robertson SJ, Haddock E, Feldmann F, Hanley PW, Scott DP, et al. VSV-EBOV rapidly protects macaques against infection with the 2014/15 ebola virus outbreak strain. *Science*. (2015) 349:739–42. doi: 10.1126/science.aab3920

28. Marzi A, Engelmann F, Feldmann F, Haberthur K, Shupert WL, Brining D, et al. Antibodies are necessary for rVSV/ZEBOV-GP-mediated protection against lethal ebola virus challenge in nonhuman primates. *Proc Natl Acad Sci USA*. (2013) 110:1893–8. doi: 10.1073/pnas.1209591110

29. Feldmann H, Jones SM, Daddario-DiCaprio KM, Geisbert JB, Ströher U, Grolla A, et al. Effective post-exposure treatment of ebola infection. *PLOS Pathogens*. (2007) 3:e2. doi: 10.1371/journal.ppat.0030002

30. Marzi A, Hanley PW, Haddock E, Martellaro C, Kobinger G, Feldmann H. Efficacy of vesicular stomatitis virus–ebola virus postexposure treatment in rhesus macaques infected with ebola virus makona. *J Infect Dis*. (2016) 214:S360–6. doi: 10.1093/infdis/jiw218

31. Cross RW, Bornholdt ZA, Prasad AN, Geisbert JB, Borisevich V, Agans KN, et al. Prior vaccination with rVSV-ZEBOV does not interfere with but improves efficacy of postexposure antibody treatment. *Nat Commun*. (2020) 11:3736. doi: 10.1038/s41467-020-17446-4

32. Kennedy SB, Bolay F, Kieh M, Grandits G, Badio M, Ballou R, et al. Phase 2 placebo-controlled trial of two vaccines to prevent ebola in liberia. *N Engl J Med*. (2017) 377:1438–47. doi: 10.1056/NEJMoa1614067

33. Agnandji ST, Huttner A, Zinser ME, Njuguna P, Dahlke C, Fernandes JF, et al. Phase 1 trials of rVSV ebola vaccine in Africa and Europe. *N Engl J Med*. (2016) 374:1647–60. doi: 10.1056/NEJMoa1502924

34. Agnandji ST, Fernandes JF, Bache EB, Mba RMO, Brosnahan JS, Kabwende L, et al. Safety and immunogenicity of rVSVΔG-ZEBOV-GP ebola vaccine in adults and children in lambaréné, gabon: a phase I randomised trial. *PLOS Med*. (2017) 14:e1002402. doi: 10.1371/journal.pmed.1002402

35. Heppner DG, Kemp TL, Martin BK, Ramsey WJ, Nichols R, Dasen EJ, et al. Safety and immunogenicity of the rVSVΔG-ZEBOV-GP ebola virus vaccine candidate in healthy adults: a phase 1b randomised, multicentre, double-blind, placebo-controlled, dose-response study. *Lancet Infect Dis*. (2017) 17:854–66. doi: 10.1016/S1473-3099(17)30313-4

36. Huttner A, Dayer JA, Yerly S, Combescure C, Auderset F, Desmeules J, et al. The effect of dose on the safety and immunogenicity

of the VSV ebola candidate vaccine: a randomised double-blind, placebo-controlled phase 1/2 trial. *Lancet Infect Dis*. (2019) 15:1156–66. doi: 10.1016/S1473-3099(15)00154-1

37. Henao-Restrepo AM, Camacho A, Longini IM, Watson CH, Edmunds WJ, Egger M, et al. Efficacy and effectiveness of an rVSV-vectored vaccine in preventing ebola virus disease: final results from the guinea ring vaccination, open-label, cluster-randomised trial (Ebola Ça Suffit!). *Lancet*. (2017) 389:505–18. doi: 10.1016/S0140-6736(16)32621-6

38. Henao-Restrepo AM, Longini IM, Egger M, Dean NE, Edmunds WJ, Camacho A, et al. Efficacy and effectiveness of an rVSV-vectored vaccine expressing ebola surface glycoprotein: interim results from the guinea ring vaccination cluster-randomised trial. *Lancet*. (2015) 386:857–66. doi: 10.1016/S0140-6736(15)61117-5

39. Widdowson MA, Schrag SJ, Carter RJ, Carr W, Legardy-Williams J, Gibson L, et al. Implementing an ebola vaccine study - Sierra Leone. *MMWR Suppl*. (2016) 65:98–106. doi: 10.15585/mmwr.su6503a14

40. Legardy-Williams JK, Carter RJ, Goldstein ST, Jarrett OD, Szefer E, Fombah AE, et al. Pregnancy outcomes among women receiving rVSVΔ-ZEBOV-GP ebola vaccine during the sierra leone trial to introduce a vaccine against ebola. *Emerg Infect Dis*. (2020) 26:541–8. doi: 10.3201/eid2603.191018

41. Samai M, Seward JF, Goldstein ST, Mahon BE, Lisk DR, Widdowson A, et al. The sierra leone trial to introduce a vaccine against ebola: an evaluation of rVSVΔG-ZEBOV-GP vaccine tolerability and safety during the West Africa ebola outbreak. *J Infect Dis*. (2018) 217:S6–15. doi: 10.1093/infdis/jiy020

42. Kilmarx PH, Clarke KR, Dietz PM, Hamel MJ, Husain F, McFadden JD, et al. Ebola virus disease in health care workers–Sierra Leone, 2014. *MMWR Morb Mortal Wkly Rep*. (2014) 63:1168–71.

43. Halperin SA, Arribas JR, Rupp R, Andrews CP, Chu L, Das R, et al. Six-Month safety data of recombinant vesicular stomatitis virus-zaire ebola virus envelope glycoprotein vaccine in a phase 3 double-blind, placebo-controlled randomized study in healthy adults. *J Infect Dis*. (2017) 215:1789–98. doi: 10.1093/infdis/jix189

44. Halperin SA, Das R, Onorato MT, Liu K, Martin J, Grant-Klein RJ, et al. Immunogenicity, lot consistency, and extended safety of rVSVΔG-ZEBOV-GP vaccine: a phase 3 randomized, double-blind, placebo-controlled study in healthy adults. *J Infect Dis*. (2019) 220:1127–35. doi: 10.1093/infdis/jiz241

45. Regules JA, Beigel JH, Paolino KM, Voell J, Castellano AR, Hu Z, et al. A recombinant vesicular stomatitis virus ebola vaccine. *N Engl J Med*. (2017) 376:330–41. doi: 10.1056/NEJMoa1414216

46. Dahlke C, Kasonta R, Lunemann S, Krähling V, Zinser ME, Biedenkopf N, et al. Dose-dependent T-cell dynamics and cytokine cascade following rVSV-ZEBOV immunization. *EBioMedicine*. (2017) 19:107–18. doi: 10.1016/j.ebiom.2017.03.045

47. Backman TWH, Girke T. systemPipeR: NGS workflow and report generation environment. *BMC Bioinform*. (2016) 17:388. doi: 10.1186/s12859-016-1241-0

48. Nueda MJ, Tarazona S, Conesa A. Next maSigPro: updating maSigPro bioconductor package for RNA-seq time series. *Bioinformatics*. (2014) 30:2598–602. doi: 10.1093/bioinformatics/btu333

49. Ernst J, Bar-Joseph Z. STEM: a tool for the analysis of short time series gene expression data. *BMC Bioinform*. (2006) 7:191. doi: 10.1186/1471-2105-7-191

50. Zhou Y, Zhou B, Pache L, Chang M, Khodabakhshi AH, Tanaseichuk O, et al. Metascape provides a biologist-oriented resource for the analysis of systems-level datasets. *Nat Commun*. (2019) 10:1523. doi: 10.1038/s41467-019-09234-6

51. Frishberg A, Brodt A, Steuerman Y, Gat-Viks I. ImmQuant: a user-friendly tool for inferring immune cell-type composition from gene-expression data. *Bioinformatics*. (2016) 32:3842–3. doi: 10.1093/bioinformatics/btw535

52. Messaoudi I, Estep R, Robinson B, Wong SW. Nonhuman primate models of human immunology. *Antioxid Redox Signal*. (2011) 14:261–73. doi: 10.1089/ars.2010.3241

53. Longet S, Mellors J, Carroll MW, Tipton T. Ebolavirus: comparison of survivor immunology and animal models in the search for a correlate of protection. *Front Immunol*. (2021) 11:3871. doi: 10.3389/fimmu.2020.599568

54. Abbas AR, Baldwin D, Ma Y, Ouyang W, Gurney A, Martin F, et al. Immune response in silico (IRIS): immune-specific genes identified from a compendium of microarray expression data. *Genes Immun*. (2005) 6:319–31. doi: 10.1038/sj.gene.6364173

55. Speranza E, Connor JH. Host transcriptional response to ebola virus infection. *Vaccines*. (2017) 5:E30. doi: 10.3390/vaccines5030030

56. Menicucci AR, Versteeg K, Woolsey C, Mire CE, Geisbert JB, Cross RW, et al. Transcriptome analysis of circulating immune cell subsets highlight the role of monocytes in zaire ebola virus makona pathogenesis. *Front Immunol.* (2017) 8:1372. doi: 10.3389/fimmu.2017.01372

57. Pinski AN, Maroney KJ, Marzi A, Messaoudi I. Distinct transcriptional responses to fatal ebola virus infection in cynomolgus and rhesus macaques suggest species-specific immune responses. *Emerg Microbes Infect.* (2021) 10:1320–30. doi: 10.1080/22221751.2021.194 2229

58. Pinski A, Woolsey C, Jankeel A, Cross R, Basler CF, Geisbert T, et al. Transcriptional analysis of lymphoid tissues from infected nonhuman primates reveals the basis for attenuation and immunogenicity of an Ebola virus encoding a mutant VP35 protein. *J Virol.* (2021) 95:e01995–20. doi: 10.1128/JVI.01995-20

59. Bradfute SB, Warfield KL, Bavari S. Functional CD8+ T cell responses in lethal ebola virus infection. *J Immunol.* (2008) 180:4058–66. doi: 10.4049/jimmunol.180.6.4058

60. Baize S, Leroy EM, Georges-Courbot MC, Capron M, Lansoud-Soukate J, Debré P, et al. Defective humoral responses and extensive intravascular apoptosis are associated with fatal outcome in ebola virus-infected patients. *Nat Med.* (1999) 5:423–6. doi: 10.1038/7422

61. Menicucci AR, Jankeel A, Feldmann H, Marzi A, Messaoudi I. Antiviral innate responses induced by VSV-EBOV vaccination contribute to rapid protection. *mBio.* (2019) 10:e00597–19. doi: 10.1128/mBio.00 597-19

62. Sakabe S, Sullivan BM, Hartnett JN, Robles-Sikisaka R, Gangavarapu K, Cubitt B, et al. Analysis of CD8+ T cell response during the 2013-2016 ebola epidemic in West Africa. *Proc Natl Acad Sci USA.* (2018) 115:E7578–86. doi: 10.1073/pnas.1806200115

63. LaVergne SM, Sakabe S, Kanneh L, Momoh M, Al-Hassan F, Yilah M, et al. Ebola-Specific CD8+ and CD4+ T-cell responses in Sierra Leonean ebola virus survivors with or without post-ebola sequelae. *J Infect Dis.* (2020) 222:1488–97. doi: 10.1093/infdis/jiaa268

64. Dahlke C, Lunemann S, Kasonta R, Kreuels B, Schmiedel S, Ly ML, et al. Comprehensive characterization of cellular immune responses following ebola virus infection. *J Infect Dis.* (2017) 215:287–92. doi: 10.1093/infdis/jiw508

65. Gupta M, Mahanty S, Greer P, Towner JS, Shieh WJ, Zaki SR, et al. Persistent infection with ebola virus under conditions of partial immunity. *J Virol.* (2004) 78:958–67. doi: 10.1128/JVI.78.2.958-967.2004

66. Agrati C, Castilletti C, Casetti R, Sacchi A, Falasca L, Turchi F, et al. Longitudinal characterization of dysfunctional T cell-activation during human acute ebola infection. *Cell Death Dis.* (2016) 7:e2164. doi: 10.1038/cddis.2016.55

67. Rechtien A, Richert L, Lorenzo H, Martrus G, Hejblum B, Dahlke C, et al. Systems vaccinology identifies an early innate immune signature as a correlate of antibody responses to the ebola vaccine rVSV-ZEBOV. *Cell Rep.* (2017) 20:2251–61. doi: 10.1016/j.celrep.2017.08.023

68. Pejoski D, de Rham C, Martinez-Murillo P, Santoro F, Auderset F, Medaglini D, et al. Rapid dose-dependent natural killer (NK) cell modulation and cytokine responses following human rVSV-ZEBOV ebolavirus vaccination. *NPJ Vaccines.* (2020) 5:32. doi: 10.1038/s41541-020-0179-4

69. Wagstaffe HR, Clutterbuck EA, Bockstal V, Stoop JN, Luhn K, Douoguih M, et al. Antibody-Dependent natural killer cell activation after ebola vaccination. *J Infect Dis.* (2021) 223:1171–82. doi: 10.1093/infdis/jiz657